Physiology and Management of Sustainable Crops
https://www.sciltp.com/journals/pmsc

Article

Thermography Applied to the Assessment of *Podosphaera xanthii* Infection in Susceptible Melon Plants

Matilde Barón [1], María-Luisa Pérez-Bueno [1,2] and Mónica Pineda [1,*]

[1] Department of Stress, Development and Signaling in Plants, Estación Experimental del Zaidín, Consejo Superior de Investigaciones Científicas, C/Profesor Albareda, 1, 18008 Granada, Spain
[2] Department of Plant Physiology, Facultad de Ciencias, University of Granada, 18071 Granada, Spain
* Correspondence: monica.pineda@eez.csic.es; Tel.: +34-958181600

How To Cite: Barón, M.; Pérez-Bueno, M.-L.; Pineda, M.. Thermography Applied to the Assessment of *Podosphaera xanthii* Infection in Susceptible Melon Plants. *Physiology and Management of Sustainable Crops* **2026**, *2*(1), 2. https://doi.org/10.53941/pmsc.2026.100002

Received: 5 February 2026
Revised: 16 March 2026
Accepted: 17 March 2026
Published: 25 March 2026

Abstract: Powdery mildew, a disease caused by the biotrophic fungus *Podosphaera xanthii*, is one of the most destructive diseases affecting melon crops worldwide. This pathogen causes alterations in the physiology of the host plant even before visible symptoms appear, which in turn can be detected using non-invasive imaging techniques. In this piece of work, infrared thermography was used to evaluate the temperature dynamics of melon leaves infected with *P. xanthii* during the first 72 h after infection. Infected leaves showed a significant decrease in temperature compared to mock-controls from 18.5 hpi onwards, before the appearance of visible mycelium. This temperature difference between mock-control and *P. xanthii*-infected melon leaves remained significant throughout the experiment, suggesting a sustained disruption of water-balance regulation caused by the fungus. This imbalance could be linked to haustorium-mediated interference with stomatal function or epidermal osmotic homeostasis. Overall, these results highlight thermography as a powerful and sensitive tool for detecting early physiological responses during *P. xanthii* infection of melon leaves. Therefore, thermography could be used as a valuable complement to 'omics' and other image-based phenotyping methods, helping to provide a comprehensive view of the responses that different diseases trigger in host plants.

Keywords: Cucurbits; powdery mildew; thermal imaging

1. Introduction

Melon (*Cucumis melo* L.) is considered to be one of the most economically significant horticultural crops in Andalusia, Spain. It occupies a substantial cultivated area and contributes to both regional income and employment [1]. However, melon production faces major challenges, as those related to fungal pathogens. Thus, powdery mildew—primarily caused by *Podosphaera xanthii* or *Golovinomyces cichoracearum*—is considered one of the most damaging diseases affecting cucurbit crops worldwide [2,3]. In Andalusia, *P. xanthii* is the fungus responsible for powdery mildew in cucurbits, and its recurrent incidence causes significant losses in yield and quality [4].

P. xanthii is an obligate biotrophic fungus that produces a white, talc-like, powdery fungal mycelium that spreads epiphytically across the surface of leaves [5]. Its life cycle consists of several phases, starting with the arrival of conidia on the leaf surface. Then, a primary appressorium is formed, which penetrates through the cuticle and cell walls. Subsequently, a primary haustorium is formed. Haustoria are the true Trojan horse of *P. xanthii*, enabling the fungus to extract nutrients and manipulate the physiology of the plant. This process leads to the growth of the mycelium and, ultimately, to the formation of conidiophores and the production of new conidia to start a new life cycle [4,6–8].

During the infection process, *P. xanthii* triggers strong differential gene expression in melon plants, leading to an extensive reprogramming of metabolic pathways within the plant. Consequently, a variety of physiological processes are influenced by the fungus, including primary metabolism, phenylpropanoid biosynthesis, cellular homeostasis and defence-related pathways [2,8]. Moreover, powdery mildew can alter the anatomical and functional properties of stomata, such as stomatal density, morphology and dimensions, contributing to disruptions in leaf transpiration and water balance [9].

Assessing plant physiology is a laborious task involving the use of numerous destructive techniques and methodologies, which are often time-consuming. However, there is an alternative approach, namely plant phenotyping using image sensors. These techniques have been proven to be reliable and non-destructive, providing results in a very short time. This makes it possible to detect plant stress (such as that caused by pathogens) before symptoms become visible [10]. A variety of imaging techniques can be applied to the study of plant physiology, with each technique yielding information on different metabolic processes in plants [11]. Among these, thermography, which measures the infrared radiation, provides information about the temperature of plants. As leaf surface temperature inversely correlates to leaf transpiration, thermal imaging is a powerful, non-invasive method for evaluating stomatal behaviour and transpiration in real time [12]. Moreover, stresses that disrupt the integrity of leaves can also be detected by thermography, as they can lead to uncontrolled water loss [13]. Consequently, thermography has become an essential component in high-throughput phenotyping platforms, enabling the assessment of stomatal regulation, plant stress responses, and water-use traits under both controlled and field conditions [14,15]. Several recent reviews summarize studies reporting pathogen infections detected using this approach [16,17]. A recent example shows that infection caused by the fungus *Fusarium graminearum* in wheat can be successfully detected using high-throughput phenotyping platforms incorporating thermal cameras [18].

Polonio et al. [2] evaluated the effect of *P. xanthii* infection on susceptible melon plants, relating the quantified transcriptional changes caused by the infection with those observed by sensors providing information on photosynthesis and secondary metabolism. However, no thermal information was included. In order to expand the scope of that study, the compatible interaction of *P. xanthii*-melon leaves was evaluated by means of continuous measurement of leaf temperature using thermography. A substantial decrease in leaf temperature was observed following 18.5 h of interaction, prior to the formation of visible mycelium. The potential causes of this decline in temperature are examined in detail.

2. Material and Methods

2.1. Plant Cultivation

Melon seeds (*Cucumis melo* cv. 'Rochet Panal'; Semillas Fitó, Barcelona, Spain) were sterilised in a 20% bleach solution for 2 min. The seeds were then rinsed twice with sterile water for two minutes each time and left to germinate on filter paper moistened with sterile water at 24 °C in the dark for one week. The seedlings were then transferred to pots containing a 1:1 (*v*:*v*) mixture of soil and coconut fibre, and placed in the growth chamber under a 16/8 h light/dark photoperiod, at 22/18 ºC day/night temperature, and 65% relative humidity. The light intensity was set at 200 μmol $m^2 \cdot s^{-1}$ PAR (photosynthetic light radiation). Following a 14-day period under these conditions, the plants were inoculated with either a mock solution or the pathogen.

2.2. Podosphaera xanthii Cultivation and Inoculation

Podosphaera xanthii SF48 was cultivated on zucchini cotyledons (*Cucurbita pepo* L. cv. 'Negro Belleza'; Semillas Fitó) that had been previously disinfected (following the same protocol used for melon seeds) and kept in Bertrand medium [4% sucrose, 1% agar, 3 $mg \cdot L^{-1}$ benzimidazole (Sigma-Aldrich, San Louis, MO, USA)] at 22 °C for a period of one week.

The third true leaf of three-week-old plants was inoculated with a mock solution or a solution containing conidia of *P. xanthii*, according to [2]. Firstly, conidia of *P. xanthii* were recovered by washing infected zucchini cotyledons with 50 mL of a 0.01% aqueous solution of Tween-20 (Scharlab, Barcelona, Spain). The spore suspension was then adjusted to a final concentration of 1×10^6 conidia$\cdot mL^{-1}$ for the purpose of inoculating the melon plants, by means of spraying. In the case of the mock-control leaves, 0.01% Tween-20 was used as the spraying agent.

2.3. Thermal Imaging

Infrared images and thermographic data were collected using a FLIR A305sc camera (FLIR Systems, Wilsonville, OR, USA), mounted in a vertical position above the leaf surface. The system produced images with

a spatial resolution of 320 × 240 pixels and a thermal sensitivity < 0.05 °C, operating within a spectral window of 7.5–13 µm. Image acquisition and temperature extraction were carried out using FLIR Research & Development software (version 3.4). Thermal images were displayed with a false-colour scale and represent typical results obtained under standard experimental conditions.

In the case of discrete time-points measurements, temperature leaf was captured at 24 and 72 hours post inoculation (hpi). Individual leaves were placed 30 cm below the thermal camera and measured one by one. Images were captured of a total of 9 leaves per treatment, and three different experiments were conducted with similar results.

In the case of continuous measurements, 6 leaves (two rows of three leaves each; Figure 1) were placed at the same time 90 cm below the thermal camera, fixed with clips to avoid leaf movements, and temperature was recorded every 30 min from 0 to 72 hpi. Mock-control leaves were placed in the upper row; whereas *P. xanthii*-inoculated leaves were located in the lower row. Three different experiments were conducted yielding similar outcomes.

Figure 1. Set-up for continuous measurement of leaf temperature. This image was taken at 24 hpi (hours post inoculation). Mock-controls were positioned in the upper row, while *P. xanthii*-infected leaves were arranged in the lower row. The thermal camera was vertically fixed at a height of 90 cm above the leaves and was set to take images every 30 min.

2.4. Data Analysis

In order to obtain the temperature values of the leaves (using FLIR Research & Development software), four regions per leaf were delineated and subsequently, the temperature values in each region were extracted and averaged. Thus, for discrete time-points leaf measurements, n = 36 (9 leaves × 4 regions); and for continuous measurements, n = 12 (3 leaves × 4 regions).

In order to compare the leaf temperature of mock-control leaves and *P. xanthii*-infected leaves, Student's *t*-test was applied to the data obtained from the thermal images using Excel 2016 (Microsoft Corporation, Redmond, WA, USA). Statistically significant differences were considered at $p < 0.05$ (*), $p < 0.01$ (**) or $p < 0.001$ (***). The graphs were prepared using the Microsoft Excel 2016 software. Mean ± standard errors are displayed.

3. Results

3.1. Symptomatology

To confirm the successful establishment of a *P. xanthii* infection on melon leaves, the experiments were maintained in the growth chamber until the characteristic white, talcum powder-like fungal mycelium appeared on the leaf surface. However, thermal measurements were taken up to 72 hpi, while the symptoms remained invisible to the naked eye (Figure 2, RGB panels). It is therefore interesting to note that all alterations caused by the fungus in leaf temperature were presymptomatic.

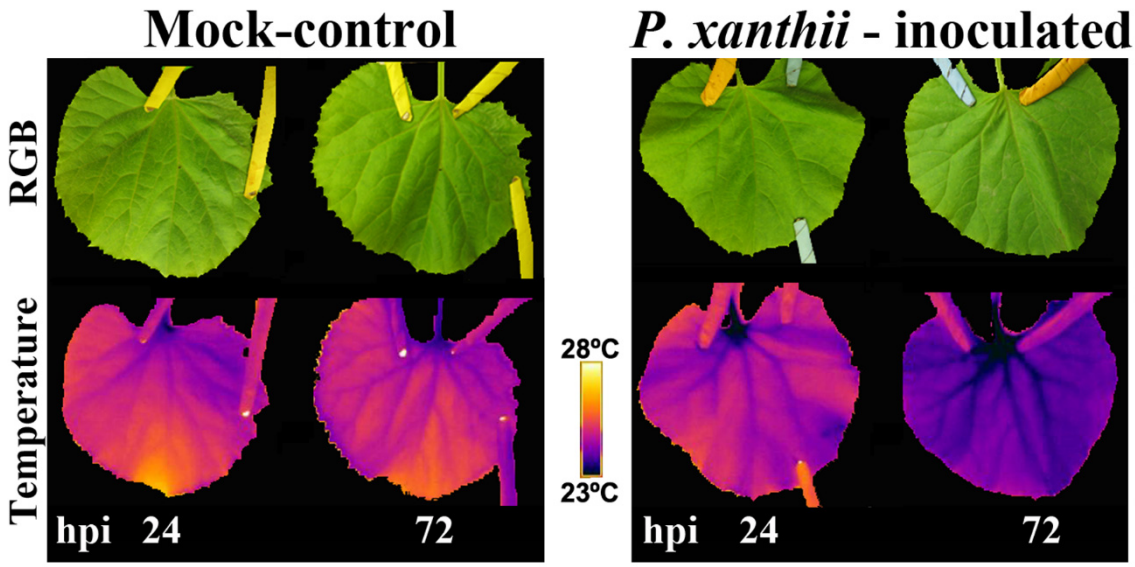

Figure 2. Real (RGB) and thermal images (temperature) of both mock-control and *P. xanthii*-infected leaves after 24 and 72 hours post inoculation (hpi). A false colour scale has been applied to the thermal images, and the temperature scale is displayed in the image. Representative images of each treatment are shown.

3.2. Leaf Temperature after 24 and 72 h Post Inoculation

To determine the effect of *P. xanthii* on melon leaves transpiration, temperature of the leaves was obtained by means of a thermal camera after 24 and 72 hpi (Figure 2, Temperature panel; Figure 3).

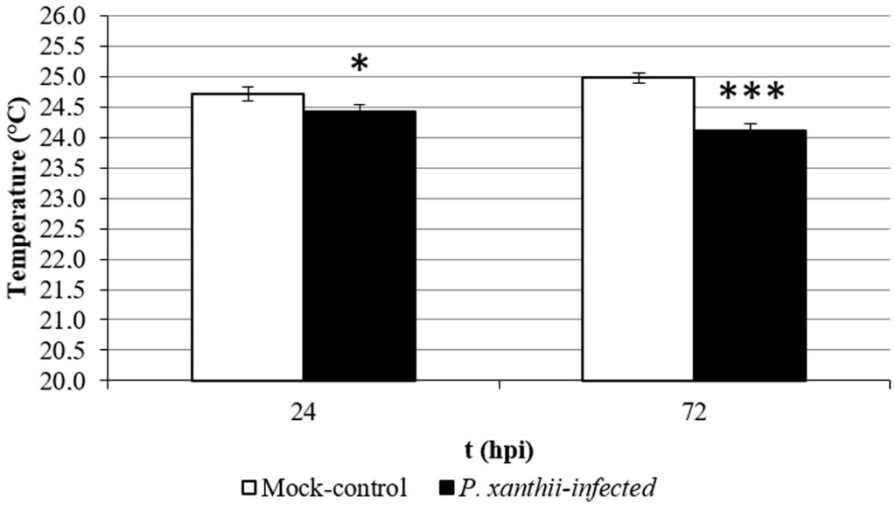

Figure 3. Temperature values of mock-control (white bars) and *P. xanthii*-infected (black bars) melon leaves after 24 and 72 hours post inoculation (hpi) obtained from images recorded by the thermal camera. Significant differences were displayed at $p < 0.05$ (*) and $p < 0.001$ (***), according to a Student's *t* test. N = 36. Mean ± standard errors are shown.

Significant differences in leaf temperature were recorded between *P. xanthii*-infected melon leaves and the mock-controls at both 24 and 72 hpi (0.28 °C and 0.87 °C, respectively), confirming a sustained cooling effect in the infected leaves.

3.3. Continuous Measurement of Melon Leaf Temperature

To try to elucidate when exactly the decrease in temperature occurred in melon leaves infected with *P. xanthii*-infected melon compared to the mock-controls, experiments were designed in which the leaf temperature was measured every 30 min immediately after inoculation (Figure 4).

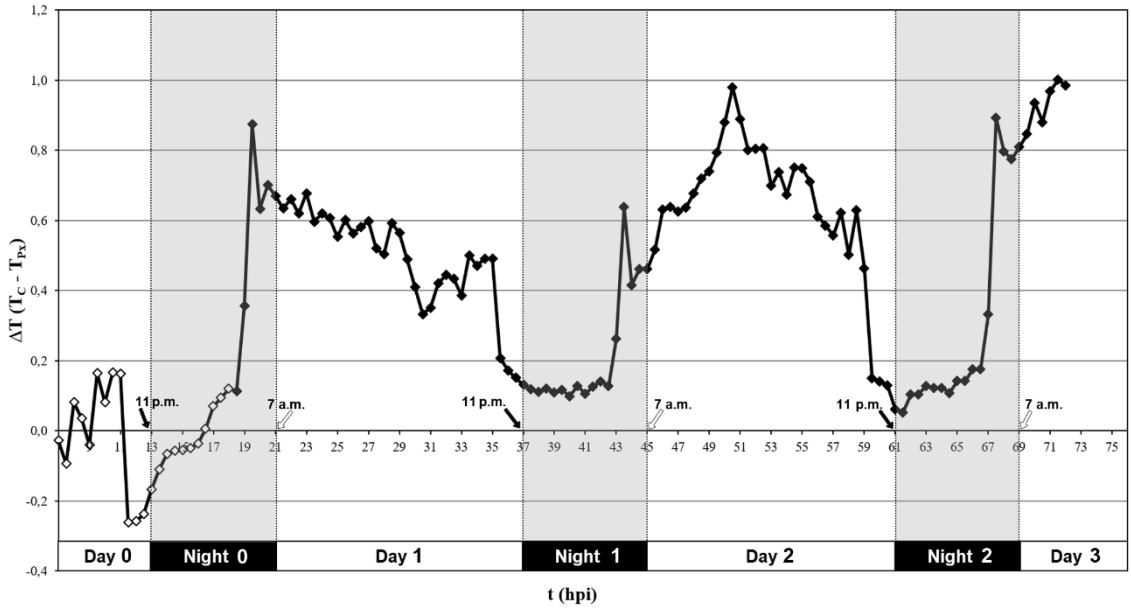

Figure 4. Temperature difference (ΔT) between leaves of mock-control plants (T_C) and leaves from plants infected with *Podosphaera xanthii* (T_{PX}) during 72 hours post inoculation (hpi), as shown in X-axis. The plants were placed in the growth chamber, where periods of light (white boxes) and darkness (grey boxes) followed each other, simulating day/night conditions. Plants were inoculated at 10 a.m. (corresponding at 0 hpi) in the day 0. Night conditions started at 11 p.m. every day (black arrows), whereas day conditions started at 7 a.m. every day (white arrows). Open symbols (◊) denote non-significant differences, whereas black symbols (♦) indicate significant differences at $p < 0.05$.

Figure 4 shows the temperature difference (ΔT) between the mock-control and *P. xanthii*-infected leaves of plants placed in the growth chamber. Temperature was registered every 30 min from 7 hpi until the end of the experiment at 72 hpi. In the growth chamber, daytime conditions began at 7 a.m. (white boxes, Figure 4), while night-time mode began at 11 p.m. (grey boxes, Figure 4). Plants were inoculated at 10 a.m. on day 0; this time of day corresponds to 0 hpi. As the leaves were inoculated by spraying the spore vehicle solution, and the evaporation of the inoculum droplets caused an artefactual decrease in temperature of both the mock-control leaves and those infected with *P. xanthii*, the first 6.5 h (the time it took for the inoculum to evaporate) are not shown in Figure 4. Until 18 hpi, no significant differences in leaf temperature between treatments were found; however, from 18.5 h onwards, the leaf temperature was significantly higher for the mock-control leaves than for the leaves infected by the fungus, as the values of ΔT were positive. During nights 1 and 2, ΔT is lower than during days, because the plants actively close stomata during nights. Despite this, the differences between the mock-control and *P. xanthii*-infected leaves remained significant, suggesting that another factor is involved in the process of water balance regulation.

4. Discussion

A key challenge in plant–pathogen interaction research is to understand how pathogens reprogram host physiology during the earliest stages of infection [19]. In the case of compatible interactions, physiological and molecular changes frequently occur prior to the appearance of visible symptoms, but they may be difficult to identify as these responses are often subtle, spatially restricted, and overlap with general stress- and homeostasis-related processes [19,20]. Non-invasive imaging techniques allow these early alterations to be captured in real time and linked to the underlying physiological processes [10]. In this regard, thermography is an effective way of detecting changes in the water relations of leaves associated with pathogen colonisation. Thermography has been extensively validated as a reliable, rapid indicator of transpiration and stomatal conductance, as leaf temperature shows an inverse correlation with both processes [13]. For this reason, thermal imaging was used in this study rather than other techniques, such as infrared gas analyser measurements, to determine whether *P. xanthii* manipulates the water balance of melon leaves to its advantage.

When analysed by means of thermography under ambient controlled conditions, such as those used in the experiments, *P. xanthii*-infected melon leaves displayed a decline in temperature respecting to the mock-controls. This decrease was significant from 18.5 hpi, well before the appearance of visible white mycelium. Similar

presymptomatic thermal signatures have been reported for powdery mildew and other fungal diseases in different host species, supporting the use of thermal imaging as an early indicator of plant–pathogen interactions [13,21–23].

Early cooling caused by water loss is consistent with a presymptomatic physiological disturbance associated with *P. xanthii* colonization. Water balance, a key determinant of plant homeostasis [24], is mainly controlled by stomata, whose behaviour is finely tuned [25]. Nevertheless, some pathogens have been found to manipulate the stomatal apparatus to their own advantage [26]. For instance, rust fungi use stomata to penetrate and feed on the host plant. The penetrating hyphae form a physical barrier that prevents the stomata from closing properly, resulting in water loss and cooling of the leaf in the earliest phases of infection [27,28]. However, it is well known that *P. xanthii* does not use stomata to penetrate host cells, suggesting that no physical barriers disturb the degree of aperture of melon leaf stomata. Instead, *P. xanthii* develops a haustorium: a specialised feeding structure surrounded by a plant-derived extrahaustorial membrane that enables nutrient uptake and effector delivery while keeping the host cell alive [2,7]. Furthermore, although haustorial penetration involves substantial remodelling of the host cell membrane, ultrastructural and cell biological studies have demonstrated that host cell integrity is largely preserved during the formation of the extrahaustorial membrane. Therefore, extensive passive water leakage due to physical damage is an unlikely explanation for the observed cooling [7,29].

Plants have developed defence mechanisms to control water loss through transpiration caused by pathogens [30,31]. For instance, abscisic acid-mediated responses are commonly associated with stomatal closure during biotic stress [32]. In the case of a *P. xanthii* infection, the expression levels of genes related to the response to the abscisic acid stimulus are increased in infected melon plants [2]. On the other hand, biotrophic pathogens have been shown to interfere with or fine-tune plant signalling networks, potentially altering the functional outcome of hormone activation at the stomatal level [31,33]. In this case, haustoria of *P. xanthii* would act as potent metabolic sinks, depleting solutes from the host epidermis and disrupting the osmotic balance required for stomatal control. This manipulation may override the plant's stomatal closure signals, resulting in an atypical increase in transpiration during the compatible interaction [26], even at night, when stomata naturally close. However, further experiments will be required to elucidate the specific mechanisms underlying the observed thermal effects, such as microscopic observations, biochemical analyses of defence-related enzymes, metabolomics, and other approaches.

5. Conclusions

The decrease in temperature of *P. xanthii*-infected leaves compared to the mock-controls was detected presymptomatically from 18.5 hpi onwards, suggesting that *P. xanthii* could disrupt the water balance of melon leaves at an early stage. This could be a consequence of alterations in the osmotic balance of the leaf epidermal surface caused by of haustoria. However, further experiments will be required to determine the physiological basis of this response.

This study underscores the value of thermography as a highly sensitive, non-invasive approach for early disease detection. Nevertheless, detecting presymptomatic powdery mildew in the field using thermography can be challenging due to uncontrolled ambient conditions and varying infection stages. One possible approach to overcome this limitation involves using high-throughput phenotyping platforms or drone-based thermographic imaging combined with artificial intelligence algorithms trained to classify leaves as healthy or infected. Subsequent selective validation via visual inspection or molecular assays would allow accurate field-scale detection.

Author Contributions

M.P. and M.-L.P.-B. performed the experiments. M.P. analysed the data, prepared figures and wrote the manuscript. M.B. obtained the funds and revised different versions of the manuscript. All authors have read and agreed to the published version of the manuscript.

Funding

This work was supported by a grant from CICE-Junta de Andalucía (P12-AGR-0370), and Ministerio de Economía y Competitividad-CSIC and ERDF funds (RECUPERA 2020/20134R060); and grant PID2022-139733OB-I00 funded by MICIU/AEI/10.13039/501100011033 and by "ERDF A way of making Europe" by ERDF/EU. MICIU: Spanish Ministerio de Ciencia, Innovación y Universidades; AEI: Agencia Estatal de Investigación; ERDF: European Regional Development Fund from the European Union.

Institutional Review Board Statement

Not applicable. This study did not involve humans or animals requiring ethical approval.

Informed Consent Statement

Not applicable.

Data Availability Statement

The data will be made available upon reasonable request to the corresponding author.

Acknowledgments

The authors would like to thank Alejandro Pérez-García and Antonio de Vicente (IHSM-UMA, Málaga, Spain) for kindly providing the Podosphaera xanthii SF48 pathogen.

Conflicts of Interest

The authors declare no conflict of interest. Given the role as a member of the Editorial Board, Mónica Pineda had no involvement in the peer review of this paper and had no access to information regarding its peer-review process. Full responsibility for the editorial process of this paper was delegated to another editor of the journal.

Use of AI and AI-Assisted Technologies

The authors used DeepL (www.deepl.com) for improving language editing. Following the utilisation of this tool, the authors conducted a thorough review and edit of the content, taking full responsibility for the final version of the manuscript.

References

1. Andalucía, J.d. Principales datos de melón: Campañas 2016/17–2020/21. Consejería de Agricultura, Pesca, Agua y Desarrollo Rural. Observatorio de Precios y Mercados 2021; pp. 1–7. Available online: https://ws142.juntadeandalucia.es/agriculturaypesca/observatorio/servlet/FrontController?ec=default&action=DownloadS&table=11114&element=3939741&field=DOCUMENTO (accessed on 22 January 2026).
2. Polonio, Á.; Pineda, M.; Bautista, R.; et al. RNA-seq analysis and fluorescence imaging of melon powdery mildew disease reveal an orchestrated reprogramming of host physiology. *Sci. Rep.* **2019**, *9*, 7978.
3. Bellón-Gómez, D.; Vela-Corcia, D.; Pérez-García, A.; et al. Sensitivity of *Podosphaera xanthii* populations to anti-powdery-mildew fungicides in Spain. *Pest Manag. Sci.* **2015**, *71*, 1407–1413.
4. Martínez-Cruz, J.; Romero, D.; de Vicente, A.; et al. Transformation of the cucurbit powdery mildew pathogen *Podosphaera xanthii* by *Agrobacterium tumefaciens*. *New Phytol.* **2017**, *213*, 1961–1973.
5. Keinath, A.P.; Wintermantel, W.M.; Zitter, T.A. *Compendium of cucurbit diseases and pests, Second Edition*; APS Press: St. Paul, MN, USA, 2017; pp. 62–64.
6. Cao, Y.; Diao, Q.; Chen, Y.; Jin, H.; Zhang, Y.; Zhang, H. Development of KASP markers and Identification of a QTL underlying powdery mildew resistance in melon (*Cucumis melo* L.) by bulked segregant analysis and RNA-Seq. *Front. Plant Sci.* **2021**, *11*, 593207.
7. Martínez-Cruz, J.; Romero, D.; Dávila, J.C.; Pérez-García, A. The *Podosphaera xanthii* haustorium, the fungal Trojan horse of cucurbit-powdery mildew interactions. *Fungal Genet. Biol.* **2014**, *71*, 21–31.
8. Polonio, Á.; Seoane, P.; Claros, M.G.; et al. The haustorial transcriptome of the cucurbit pathogen *Podosphaera xanthii* reveals new insights into the biotrophy and pathogenesis of powdery mildew fungi. *BMC Genom.* **2019**, *20*, 543.
9. Tian, M.; Yu, R.; Yang, W.; et al. Effect of powdery mildew on the photosynthetic parameters and leaf microstructure of melon. *Agriculture* **2024**, *14*, 886.
10. Barón, M.; Pineda, M.; Pérez-Bueno, M.L. Picturing pathogen infection in plants. *Z. Naturforschung C* **2016**, *71*, 355–368.
11. Mahlein, A.-K. Plant disease detection by imaging sensors—Parallels and specific demands for precision agriculture and plant phenotyping. *Plant Dis.* **2016**, *100*, 241–251.
12. Jones, H.G. Application of thermal imaging and infrared sensing in plant physiology and ecophysiology. In *Advances in Botanical Research*; Academic Press: Cambridge, MA, USA, 2004; Volume 41, pp. 107–163.
13. Pineda, M.; Barón, M.; Pérez-Bueno, M.-L. Thermal imaging for plant stress detection and phenotyping. *Remote Sens.* **2021**, *13*, 68.
14. Fan, M.; Stamford, J.; Lawson, T. Using infrared thermography for high-throughput plant phenotyping. *Methods Mol. Biol.* **2024**, *2790*, 317–332.

15. Amby, D.; Westergaard, J.C.; Großkinsky, D.; et al. The PhenoLab—An automated, high-throughput phenotyping platform for analyzing development, abiotic stress responses and pathogen infection in model and crop plants. *Smart Agric. Technol.* **2025**, *11*, 100845.
16. Wen, T.; Li, J.-H.; Wang, Q.; et al. Thermal imaging: The digital eye facilitates high-throughput phenotyping traits of plant growth and stress responses. *Sci. Total Environ.* **2023**, *899*, 165626.
17. Prashar, A.; Jones, H.G. Infra-red thermography as a high-throughput tool for field phenotyping. *Agronomy* **2014**, *4*, 397–417.
18. Matkovskyi, R.; Taran, O.; Kolomyets, Y. Principles of high-throughput phenotyping and sensor platforms for non-invasive research in plant protection. *Sci. J. Biol. Syst. Theory Innov.* **2025**, *16*, 23–36.
19. Jones, J.D.G.; Dangl, J.L. The plant immune system. *Nature* **2006**, *444*, 323–329.
20. Dodds, P.N.; Rathjen, J.P. Plant immunity: Towards an integrated view of plant–pathogen interactions. *Nat. Rev. Genet.* **2010**, *11*, 539–548.
21. Jafari, M.; Minaei, S.; Safaie, N. Detection of pre-symptomatic rose powdery-mildew and gray-mold diseases based on thermal vision. *Infrared Phys. Technol.* **2017**, *85*, 170–183.
22. Chaerle, L.; Hagenbeek, D.; De Bruyne, E.; et al. Thermal and chlorophyll-fluorescence imaging distinguish plant-pathogen interactions at an early stage. *Plant Cell Physiol.* **2004**, *45*, 887–896.
23. Oerke, E.C.; Steiner, U.; Dehne, H.W.; et al. Thermal imaging of cucumber leaves affected by downy mildew and environmental conditions. *J. Exp. Bot.* **2006**, *57*, 2121–2132.
24. Torres-Ruiz, J.M.; Cochard, H.; Delzon, S.; et al. Plant hydraulics at the heart of plant, crops and ecosystem functions in the face of climate change. *New Phytol.* **2024**, *241*, 984–999.
25. Cutler, S.R.; Rodriguez, P.L.; Finkelstein, R.R.; et al. Abscisic acid: Emergence of a core signaling network. *Annu. Rev. Plant Biol.* **2010**, *61*, 651–679.
26. Melotto, M.; Zhang, L.; Oblessuc, P.R.; et al. Stomatal defense a decade later. *Plant Physiol.* **2017**, *174*, 561–571.
27. Moore, D.; Robson, G.D.; Trinci, A.P.J. *21st Century Guidebook to Fungi*, 2nd ed.; Cambridge University Press: Cambridge, NY, USA, 2020.
28. Smith, R.C.G.; Heritage, A.D.; Stapper, M.; et al. Effect of stripe rust (*Puccinia striiformis* West.) and irrigation on the yield and foliage temperature of wheat. *Field Crops Res.* **1986**, *14*, 39–51.
29. Kwaaitaal, M.; Nielsen, M.E.; Böhlenius, H.; et al. The plant membrane surrounding powdery mildew haustoria shares properties with the endoplasmic reticulum membrane. *J. Exp. Bot.* **2017**, *68*, 5731–5743.
30. Lim, C.W.; Baek, W.; Jung, J.; et al. Function of ABA in stomatal defense against biotic and drought stresses. *Int. J. Mol. Sci.* **2015**, *16*, 15251–15270.
31. Bharath, P.; Gahir, S.; Raghavendra, A.S. Abscisic acid-induced stomatal closure: An important component of plant defense against abiotic and biotic stress. *Front. Plant Sci.* **2021**, *12*, 615114.
32. Leiva-Mora, M.; Capdesuñer, Y.; Villalobos-Olivera, A.; et al. Uncovering the mechanisms: The role of biotrophic fungi in activating or suppressing plant defense responses. *J. Fungi* **2024**, *10*, 635.
33. Guan, Q.; David, L.; Moran, R.; et al. Role of *NPR1* in systemic acquired stomatal immunity. *Plants* **2023**, *12*, 2137.